Limits on the Gas Disk Content of Two "Evolved" T Tauri Stars

Alan G. Aversa

Steward Observatory, 933 N Cherry Ave., Tucson AZ 85721

ABSTRACT

We derived upper limits of the circumstellar gas disk masses around the T Tauri stars St 34 and RX J0432.8+1735 in order to place constraints on theories of planet formation and to explore the evolution of the gas-to-dust ratio during the epoch of disk dissipation around young sun-like stars. Since sub-millimeter lines of ^{12}CO trace of the cold, outer regions of circumstellar disks, we observed ^{12}CO $J = 2 - 1$ emission with the 10 m Sub-Millimeter Telescope (SMT) for two carefully chosen targets. St 34 is a rare classical T Tauri star with an age of 8 ± 3 Myr, and RX J0432.8+1735 is a rare weak-emission T Tauri star with far-infrared excess. Both exhibit radial space motion enabling us to distinguish disk emission from ambient cloud material. Assuming a ^{12}CO excitation temperature of 20 K, a ^{12}CO line-width of 5 km s^{-1}, and optically-thin emission, we derive 3σ upper limits on the H$_2$ circumstellar disk mass for St 34 and RX J0432.8+1735 to be < 4.20 M$_\oplus$ for both disks. Placing these results in the context of other studies, we discuss their implications on planet formation models.

1. Introduction

Circumstellar disks of gas and dust, a natural result of the conservation of angular momentum, are a common outcome of the star formation process. Kenyon & Hartmann (1995) find that over half the low mass (< 2 M$_\odot$) pre–main-sequence T Tauri stars in the Taurus-Auriga star formation region have more infrared emission than expected from a normal stellar photosphere, indicating the presence of a dusty circumstellar disk heated by the parent star as well as active accretion. T Tauri stars fall into two categories: Weak-Line T Tauri Stars (WTTSs), characterized by low Hα equivalent widths, and Classical T Tauri Stars (CTTSs), with higher Hα equivalent widths indicative of ongoing gas accretion. These circumstellar disks generally have the following properties (Dutrey et al. 2007; Andrews et al. 2009): mass surface densities $\Sigma(r) \propto r^{0\,\text{to}\,-1.0}$, surface temperatures $T(r) \propto r^{0\,\text{to}\,-0.6}$ (depending on disk flaring), and Keplerian rotational velocities $V(r) \propto r^{0.5}$.

Gas giant planet formation depends upon the gas content of the circumstellar disk from which they form. Primordial inner disks traced by hot dust disappear after about 3 Myr with a range of $1 - 10$ Myr (Meyer et al. 2007). If gas content and dust content in disks dissipate through similar mechanisms (Damjanov et al. 2007), then we would expect gas to disappear on these same timescales. To understand the timescales of planet formation, we must understand how long a gas disk persists around its parent star. Accretion rates (higher in CTTSs than WTTSs) also trace the time evolution of gas content as gas must be present to accrete. Durisen et al. (2007) suggest that gravitational instabilities in gas disks could account for their rapid (< 3 Myr) dissipation, locking up mass in planets. In contrast, simulations of the evolution of gas disk surface density for a 1 $M_\odot$ star due to photo-evaporation indicate that gas disks disappear in about 6 Myr (Alexander et al. 2006; Dullemond et al. 2007). Because there are various theoretical results for the gas dispersal mechanisms and associated timescales, we might expect to observe diverse properties for gas disks around T Tauri stars.

Ideally, sub-millimeter interferometric images of T Tauri stars would yield the most information about circumstellar disks, including their orientation, geometry, and gas content. Yet observations of this sort have only been published for a few nearby stars (e.g., Sub-Millimeter Array (SMA) observations of TW Hya; Qi et al. 2004). Infrared photometric campaigns with *Spitzer*, such the Cores to Disks (Evans et al. 2003) and the Formation and Evolution of Planetary Systems (FEPS; Meyer et al. 2006) *Spitzer* Legacy projects, provide knowledge of the dust circumstellar disks based upon IR excesses at many wavelengths including 24μm, which trace dust within a few AU of the parent star, and at 70μm, which trace cooler dust at larger radii. Silverstone et al. (2006) surveyed 74 stars with ages between 3-30 Myr finding no stars with mid–IR excess that were not gas rich accreting T Tauri stars. Padgett et al. (2006) however identified a handful of WTTS (lacking signatures of accretion) with evidence for mid– and far–IR excess emission. Photometric IR observations do not, however, constrain the total gas content in circumstellar disks because of a potentially highly variable gas-to-dust ratio. Observing the rotational energy transitions of ^{12}CO, a proxy for molecular hydrogen (H_2), and assuming the ISM abundance ratio $[H_2/CO] \approx 10^4$ enables one to trace the majority of cold gas in disks out to radii many times larger. Is the timescale for gas dissipation similar to the timescale for dust dissipation around T Tauri stars? This is the central question we address with our new observations.

Expanding on previous works (e.g. Pascucci et al. 2006; van Kempen et al. 2007), we search for ^{12}CO $J = 2 - 1$ emission for two "evolved" T Tauri stars in Taurus to place constraints on their gas circumstellar disk masses. St 34 is evolved in the sense that it is

8 ± 3 Myr old, whereas RX J0432.8+1735 is evolved in the sense that—although it is much younger (1.0 ± 0.5 Myr)—it has already lost its inner accretion disk. In §2, we describe our selection of sources and observations, then in §3 we derive upper limits on our sources' gas disk masses. Lastly, in §4 we describe the implications of our results, and in §5 we list our conclusions.

2. Observations

2.1. Selection of Sources

We observed the ^{12}CO $J = 2 - 1$ emission of the Taurus region objects St 34 and RX J0432.8+1735, T Tauri stars with known 24 or 70μm excesses (Kenyon & Hartmann 1995; Padgett et al. 2006, see Table 1). In order to detect gas in their circumstellar disks, we must be able to distinguish emission from the disk and surrounding molecular cloud. From available candidate "evolved" (in age or shape of spectral energy distribution) T Tauri stars, we selected those least likely to be contaminated by the ambient CO emission from the parent molecular cloud based on the Dame et al. (1987) CO survey. The radial velocities of our sources differ from the systemic velocities of any CO emission in the vicinity of our sources by $\sim 2 - 3$ km s^{-1}.

2.1.1. St 34

St 34 (HBC 425) is a binary system of two CTTSs, separated by $\lesssim 0.78$ AU (White & Hillenbrand 2005) based on the orbital solution for the system (Downes & Keyes 1988) in the Taurus-Auriga T association (Kenyon & Hartmann 1995). Both components of the spectroscopic binary have roughly equal mass and spectral types of M3 (White & Hillenbrand 2005). White & Hillenbrand (2005) observed St 34 in the optical with the HIRES spectrograph at Keck and derived an isochronal age of 8 ± 3 Myr for both components of the binary. Since they did not detect any lithium (^{7}Li) in the spectrum, St 34 must have reached—assuming the stars are completely convective—an internal temperature $> 2 \times 10^6$ K and since depleted all of its lithium. St 34 has a low accretion rate of 2.5×10^{-10} M$_\odot$ yr^{-1}, and the maximum radial velocity difference between the two binary components of St 34 is 58.4 km s^{-1} (White & Hillenbrand 2005). St 34, being one of the oldest known pre–main-sequence (PMS) star still accreting from a proto-planetary disk, also has a low dust mass of $\sim 2 \times 10^{-10}$ M$_\odot$ for radii $\lesssim 0.7$ AU (Hartmann et al. 2005).

Table 1.   Candidate Source Summary

Object	α (J2000)	δ (J2000)	Heliocentric RV (km s^{-1})	Source V_{LSR}[a] (km s^{-1})	Cloud V_{LSR}[b] (km s^{-1})	T_{eff} (K)	$\log L^{\star}$ ($\log L_{\odot}$)	Mass ($M_{\odot}$)	Age (Myr)	General Reference
RX J0432.8+1735	04 32 53.23	17 35 33.68	18.6	7.3	10.2	3499[c]	$\sim -6.1 \times 10^{-2}$[g]	$\cdots$	1 ± 0.5[d]	a
St 34	04 54 23.70	17 09 54.00	17.9 ± 0.6	6.6	8.37	3415	1.03 ± 0.06	0.37 ± 0.08[e]	8 ± 3[e,f]	b

References. — For RVs, see Wichmann et al. (2000); White & Hillenbrand (2005). For general references, see (a) Padgett et al. (2006) and (b) White & Hillenbrand (2005).

[a]We corrected the heliocentric radial velocities (RVs) from the literature into local standard of rest (V_{LSR}) radial velocities assuming the sun moves toward J2000 ($\alpha = 18^{\mathrm{h}}0, \delta = 30°0$) at 20 km s^{-1}.

[b]Determined by the ^{12}CO $J = 1 - 0$ emission from the Dame et al. (1987) survey

[c]Wichmann et al. (2000)

[d]D'Antona & Mazzitelli (1997)

[e]For both binary components

[f]Isochronal age is given. The Li depletion age for both binary components is > 25 Myr.

[g]Estimated by integrating the spectral energy distribution (SED) of RX J0432.8+1735 in Padgett et al. (2006)

2.1.2. RX J0432.8+1735

RX J0432.8+1735 is a WTTS of spectral type M2 (Martín & Magazzù 1999). Based on the PMS tracks of D'Antona & Mazzitelli (1997) RX J0432.8+1735 is estimated to be 1.0 ± 0.5 Myr old. Padgett et al. (2006) observed RX J0432.8+1735 with *Spitzer* and noticed that its 24μm flux is in excess of the expected photospheric value by a factor of 3. Its lack of IR excess $\leq 12\mu$m suggests there may be a large inner hole in the disk. Based on *ROSAT* observations, Carkner et al. (1996) discovered that RX J0432.8+1735 is also an X-ray source. As RX J0432.8+1735 is classified as a WTTS star with no estimates of its accretion rate, we assume it is not accreting.

2.2. Observing Procedure

On 26-27 November 2007, we observed the ^{12}CO $J = 2 - 1$ (230.53799 GHz) emission line of our two T Tauri stars with the 10 m Heinrich Hertz Sub-Millimeter Telescope (HHT) on Mt. Graham, Arizona. Observations were obtained with a 1 mm dual polarization (Vpol, Hpol), sideband-separating, ALMA prototype receiver. The upper sideband was tuned to ^{12}CO $J = 2 - 1$ while the lower sideband was tuned to ^{13}CO $J = 2 - 1$. We used the Forbes Filter Bank (FFB) backend in 4 IF mode, an upper and lower sideband each with 1 MHz and 250 kHz of spectral resolution, respectively. The channel width, $\Delta\nu_{\rm ch}$, of our spectrometer was 0.33 km s^{-1}. The 1 MHz resolution data were used to determine main beam efficiencies $\eta_{\rm mb}$, and the 250 kHz resolution data were used to measure the ^{12}CO line.

Using CLASS in the GILDAS data reduction package, we estimated the main beam efficiencies by observing the planets shown in Table 2. Typical sideband rejections, ignored in the calibration, were > 10 dB. The main beam efficiency η was computed following Mangum (1993) and corrected for single-sideband observations:

$$\eta = \frac{T_A^\star(\text{planet})}{J(\nu_s, T_{\text{planet}}) - J(\nu_s, T_{\text{cmb}})} \times \left[1 - \exp\left(-\ln(2)\frac{\theta_{\rm eq}\theta_{\rm pol}}{\theta_{\rm mb}^2}\right)\right]^{-1}, \tag{1}$$

where

$$J(\nu, T_b) = \frac{h\nu/k}{e^{\frac{h\nu}{kT_{\rm mb}}} - 1} \tag{2}$$

is the Planck function at brightness temperature T_b and frequency ν, $T_A^\star$ is the single-sideband antenna temperature of the planet, T_{planet} is the planet's observed brightness temperature, $T_{\rm cmb} = 2.73$ K, $\theta_{\rm eq}$ and $\theta_{\rm pol}$ are respectively the planet's equatorial and

poloidal diameters in arcseconds, and $\theta_{\mathrm{mb}} = 33''$ at $\nu = 230$ GHz. We adopted an average Venus brightness temperature T_b from Kuznetsov et al. (1982) of 287 ± 20 K. For all other planets' T_b, we used the JCMT online database[1]. We derived a ratio $\eta_{\mathrm{Vpol}}/\eta_{\mathrm{Hpol}}$ of the two IF's mean main beam efficiencies for both nights of 1.24 ± 0.04. We used this ratio to scale the Hpol polarization's antenna temperature up to match the level of the Vpol polarization's antenna temperature. After fitting a baseline to each spectrum, we averaged the sum of the scaled Hpol brightness temperatures and the Vpol brightness temperatures: $\frac{1}{2} \langle T_A^\star(\mathrm{Hpol, scaled}) + T_A^\star(\mathrm{Vpol}) \rangle = T_A^\star(\mathrm{sum})$. Thus we computed the corrected main beam temperature as

$$T_{\mathrm{mb}} = \frac{T_A^\star(\mathrm{sum})}{\eta_{\mathrm{Vpol}}}. \tag{3}$$

The average beam efficiencies were $\langle \eta_{\mathrm{Hpol}} \rangle = 0.68 \pm 0.01$ and $\langle \eta_{\mathrm{Vpol}} \rangle = 0.88 \pm 0.01$ for both nights.

Since we had null detections for our two sources, we must assume a line-width to calculate upper limits on the integrated intensity. We assumed typcial a line-width of $\Delta\nu = 10$ km s^{-1} ($= 7.69$ MHz). If we assume the CO line is well described by a Gaussian line shape, then the uncertainty in the integrated intensity is given by

$$\sigma_I = \sigma_{T_{\mathrm{mb}}} \sqrt{\frac{3\Delta\nu_{\mathrm{ch}}\Delta\nu}{\sqrt{\ln 2}}}, \tag{4}$$

where σ_I and Δv are the CO line fluxes and the the full width at half maximum (FWHM) and Δv_{ch} is the channel spacing 0.33 km s^{-1}; see Appendix I of Schlingman et al. (in prep.). The observations are summarized in Table 3.

3. Results & Analysis

The main-beam corrected spectra of our observations are shown in Figure 1.

While $9'$ is a rough spatial scale for comparison to the $33''$ beam of the SMT, and since we did not detect a ^{12}CO line in any of our sources, the on-cloud results from SMT are consistent with Dame et al. (1987). It is unlikely that high spatial frequency variations of $33''$ scales over $9'$ regions have systemic velocity shifts of 2-3 km^{-1}

Since we did not detect any ^{12}CO line, we convert our 3σ noise into an upper limit on the flux. A knowledge of the flux will enable us to estimate upper limits on gas disk mass.

---

[1]http://www.jach.hawaii.edu/jac-bin/planetflux.pl

Table 2.   Observation of Main Beam Efficiencies η

Planet	η_{Vpol}	η_{Hpol}	$\eta_{\mathrm{Vpol}}/\eta_{\mathrm{Hpol}}$
Mars[a]	0.80 ± 0.05	0.72 ± 0.04	1.10 ± 0.09
Mars	0.80 ± 0.05	0.71 ± 0.04	1.12 ± 0.09
Saturn	0.93 ± 0.04	0.70 ± 0.03	1.33 ± 0.08
Saturn	0.94 ± 0.04	0.69 ± 0.03	1.36 ± 0.09
Venus	0.89 ± 0.03	0.66 ± 0.03	1.35 ± 0.08
Venus	0.88 ± 0.03	0.66 ± 0.03	1.34 ± 0.08
Mars	0.87 ± 0.05	0.66 ± 0.04	1.31 ± 0.10
Mars[b]	0.87 ± 0.05	0.66 ± 0.04	1.33 ± 0.10
Mars[c]	0.88 ± 0.05	0.68 ± 0.04	1.29 ± 0.10
Mars	0.89 ± 0.05	0.68 ± 0.04	1.31 ± 0.11
Mars	0.84 ± 0.04	0.70 ± 0.04	1.21 ± 0.10
Mars	0.88 ± 0.05	0.68 ± 0.04	1.29 ± 0.10
Venus	0.93 ± 0.03	0.68 ± 0.03	1.38 ± 0.09

[a]All Mars brightness temperature errors assumed to be 5%

[b]End of first night
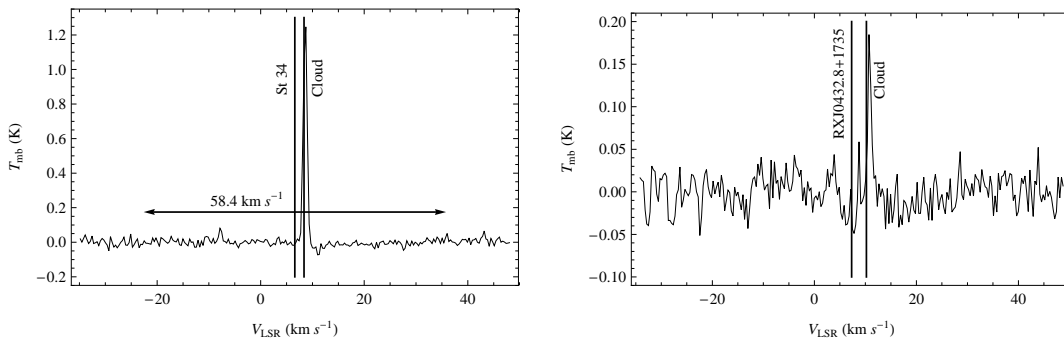
[c]Beginning of second night

Fig. 1.— Spectra of St 34 (*left*) and RX J0432.8+1735 (*right*). The vertical line labeled "Cloud" represents the estimated background cloud velocity determined by the Dame et al. (1987) CO $J = 1 - 0$ survey, and the vertical line labeled with the source's name indicates that source's V_{LSR}. For St 34, we show with an arrow the difference between the radial velocities of its binary components with an arrow centered on the systemic velocity.

<div align="center">Table 3.   Observational Summary</div>

Source	Integration Time (sec)	$\sigma_{T_{\mathrm{mb}}}$ (K)	σ_I (K km s^{-1})	$\log_{10}(F_\nu)$ ($\log_{10}$ (W cm^{-2}))	$\overline{N}(T\mathrm{ex} = 10, 20, 100$ K$)$ (10^{13} cm^{-2})	$M_{\mathrm{H}_2}(T_\mathrm{ex} = 10, 20, 100$ K$)$ (M$_\oplus$)
RX J0432.8+1735	3600	0.019	0.046	< -23.02	$< 12.7, 7.47, 6.53$	$< 3.59, 1.10, 1.84$
St 34	6120	0.019	0.046	< -23.02	$< 12.7, 7.47, 6.53$	$< 3.59, 1.10, 1.84$

Note. — T_{mb} is the main beam corrected brightness temperature and I is the corresponding intensity assuming a line width of 5 km s^{-1}. F is the 3σ line flux upper limit.

Note. — That $\sigma_{T_{\mathrm{mb}}}$ for both objects is the same is a fluke.

The observed flux is the double-integral of the observed intensity I_ν over frequency ν and solid angle Ω:

$$F = \int \int I_\nu \, d\nu \, d\Omega = \int \int \frac{2k\nu^3 T_b}{c^3} \, dv \, d\Omega. \tag{5}$$

Assuming the brightness temperature does not vary substantially over the telescope beam and that the line is a Gaussian with line-width Δv, then the upper limit on the 3σ line flux F is

$$F < \frac{2k\nu^3 (3\sigma_{T_{\rm mb}})}{c^3} \frac{\pi\theta^2}{4\ln 2} \sqrt{\frac{4\ln 2}{\pi}} \times \Delta v = (5.05 \times 10^{-15})\sigma_{T_{\rm mb}} {\rm erg\ s}^{-1}\ {\rm cm}^{-2}. \tag{6}$$

The 3σ upper limits on F are listed in Table 3.

Similarly, we can derive the column density in the optically thin limit to be

$$\overline{N}(T_{\rm ex}) = \frac{8\pi k\nu^2}{hc^3 g_u A_{ul}} \mathcal{F}(T_{\rm ex}, E_u, \nu) \int T_{\rm mb} \, dv, \tag{7}$$

where

$$\mathcal{F}(T_{\rm ex}, E_u, \nu) \equiv \frac{J_\nu(T_{\rm ex})Q(T_{\rm ex}) \exp\left(\frac{E_u}{kT_{\rm ex}}\right)}{J_\nu(T_{\rm ex}) - J_\nu(T_{\rm cmb})}, \tag{8}$$

A_{ul} is the Einstein A coefficient (spontaneous emission) and has units of s^{-1}.

Similar to the analysis of Pascucci et al. (2006), we assume an excitation temperature $T_{\rm ex} \approx 20$ K. Then in our case for ^{12}CO $J = 2 - 1$, $\mathcal{F}(T_{\rm ex}, E_u, \nu) \approx 28.00$. The Einstein $A_{ul} = 6.91 \times 10^{-7}$ s^{-1} and partition function $Q(20\ {\rm K}) = 15.9$ (CDMS[2]).

We compute and tabulate in Table 3 the ^{12}CO number densities and H$_2$ gas masses in the optically thin limit. Gas disk masses were derived from Scoville et al. (1986),

$$M_{\rm H_2} < \overline{N}(T_{\rm ex}) \times \left\{ \left[\frac{{\rm H_2}}{{\rm CO}}\right] \mu_G m_{\rm H_2} \frac{\pi\theta^2}{4} d^2 \right\} {\rm g} = 110\sigma_{T_{\rm mb}}\ {\rm M}_\oplus, \tag{9}$$

where $[{\rm H_2/CO}] \approx 10^4$, $\mu_G = 1.36$ is the mean molecular weight, $m_{\rm H_2}$ is the mass of an H$_2$ molecule, and $d \approx 140$ pc is the distance to Taurus.

4. Discussion

Theories of gaseous planet formation require knowledge of (1) how much gas there is in circumstellar disks initially and (2) the rate at which gas is depleted over time. To

---

[2]http://www.ph1.uni-koeln.de/vorhersagen/

answer the first question, upper limits on the amount of gas in very young protostellar disk systems puts limits directly on the amount of mass available for gaseous planet formation in the systems observed. Answers to the second question, requiring large samples over a wide range of ages, are also necessary because of the competition between the timescale for planet formation and gas disk dispersion timescales (for a recent review, see Meyer 2009).

There are several ways of constraining gas disk masses, each with its own advantages and disadvantages. To understand gas disk timescales, one can also analyze Hα emission line profiles and determine gas accretion rates and thus constrain the gas mass surface density at the inner edge of the disk tracing perhaps global disk evolution (e.g. Fedele et al. 2009). Using UV tracers of gas emission, Ingleby et al. (2009) describe *HST* observations searching for evidence of hot gas in emission finding no evidence for H$_2$ emission for WTTS in their sample. Ultraviolet absorption line from a continuum source (e.g. Roberge et al. 2005) can help constrain cold mass in disks, but it requires a continuum source that is bright in the far UV and an edge-on geometry; therefore, it is observationally feasible only in special circumstances. Near IR fluorescent H$_2$ traces gas with excitation temperatures $T_{\mathrm{ex}} > 2000$ K (Bary et al. 2003) and mid-IR ro-vibrational lines (e.g. Najita et al. 2007; Thi et al. 2001; Pascucci et al. 2006), especially the 28.2 μm and 17μm *Spitzer* bands, trace gas up to 50-200 K. Our observations of rotational lines of CO trace cooler gas at larger orbital radii. The disadvantage of such measurements is that CO can freeze out at the coldest temperatures corresponding to the outer limits of the disk $\gtrsim$ 30-100 AU. Hughes et al. (2010) present evidence for evolving gas to dust ratios in transitional disks which exhibit evidence for optically-thick outer disks but possess inner holes and gaps.

St 34, being 8 ± 3 Myr old, might have a lower gas surface density than typical CTTSs. It is still accreting gas (White & Hillenbrand 2005), albeit at a low rate, but retains at least a low density inner disk. Our non–detection in a search for cold gas implies that most of its outer disk must have disappeared or frozen out onto grains. White & Hillenbrand (2005) show that St 34 has an accretion rate $\langle \dot{M} \rangle = 8.3 \times 10^{-10}$ M$_\odot$ yr^{-1}, so after 1 Myr much more gas than our upper limit of 4.20 M$_\oplus$ would accrete ($\sim$ 276 M$_\oplus$). Perhaps St 34 recently lost its outer disk through photoevaporation (e.g. Gorti & Hollenbach 2009) and we are witnessing the "last gasp" of accretion onto the star. This is possible but not likely, as it requires current observations to be taking place at a very special time.

Conversely, RX J0432.8+1735—being a much younger, 1.0 ± 0.5 Myr WTTS—must have either evaporated its disk or formed planets from its gas disk faster than normal. Its being a WTTS is consistent with our null detection of its gas content, although remnant amounts of gas less than a few $M_\oplus$ could still exist in its outer disk. That RX J0432.8+1735 is relatively young and does not have detectable gas content could be significant considering

that there are older systems, such as Hen 3-600, a binary system at between $1 - 10$ Myr of age with apparent WTTS and CTTS components (Jayawardhana et al. 1999); TW Hya, a CTTS at 8-10 Myr (Webb et al. 1999); and DM Tau at ~ 8 Myr (Guilloteau & Dutrey 1994). Thus something about the disk evaporation physics is dramatically different in RX J0432.8+1735 than these oldest systems.

In Figure 2 we compare our sources' gas disk masses and ages with the gas mass upper limits of those sources ≤ 30 Myr from Pascucci et al. (2006) and with the gas mass determinations (*solid circles*) of BP Tau (^{13}CO $J = 2 - 1$; Dutrey et al. 2003); DL Tau, DO Tau (^{12}CO $J = 2 - 1$; Koerner & Sargent 1995); and DM Tau, DR Tau, GG Tau a, GM Aur, GO Tau, LkCa 15, RY Tau (^{12}CO $J = 3 - 2$ and ^{13}CO $J = 3 - 2$; Thi et al. 2001). We note that this is not an exhaustive compilation from the literature, but representative of recent results. Assuming a 1:10 gas-to-dust ratio (D'Alessio et al. 2005), we would expect RX J0432.8+1735 and St 34 to have at most 0.420 $M_{\oplus}$ and 0.420 $M_{\oplus}$ of dust, respectively, for $T_{\mathrm{ex}} = 20$ K. For St 34, Hartmann et al. (2005) estimates a disk mass of 665 $M_{\oplus}$ located in a circumbinary disks between the "wall" (the region defined to surround the two components of the St 34 binary; ~ 0.7 AU) and 7 AU. Assuming this mass is representative of a total disk mass in St 34 out to 7 AU, this would be consistent with a small (< 10 AU), optically-thick CO disk with a gas-to-dust ratio of ~ 100; we do not detect this due to beam dilation (cf. Pascucci et al. 2006).

St 34 has infrared excess for wavelengths longer than 3.6 μm (Hartmann et al. 2005) and RX J0432.8+1735 has infrared excess for wavelengths longer than 24 μm (Padgett et al. 2006), yet St 34 is a binary CTTS with an accreting inner disk and RX J0432.8+1735 is a WTTS. Binaries tend to disrupt inner gas disks (Jensen 1996) and may decrease disk lifetimes (Monin et al. 2007). However, Armitage & Clarke (1996) have argued that close binaries affect angular momentum exchange in the natural evolution of accretion disks resulting in longer lived outer disks. Indeed Thébault et al. (2004) find that planet formation around binaries might require a long-lived but massive disk. Since circumbinary disks allow for long gas disk lifetimes, St 34 might have had more time to form planets.

5.   Conclusions

Assuming optically thin disks ($\tau \ll 1$), an excitation temperature $T_{\mathrm{ex}} = 20$ K, and a line-width $\Delta v = 10$ km s^{-1}, we do not detect significant amounts of gas around three T Tauri stars: < 4.20 $M_{\oplus}$ for the PMS binary St 34 and < 4.20 $M_{\oplus}$ for RX J0432.8+1735. St 34, a CTTS, is still accreting gas although it is 8 ± 3 Myr old, and the gas disk of
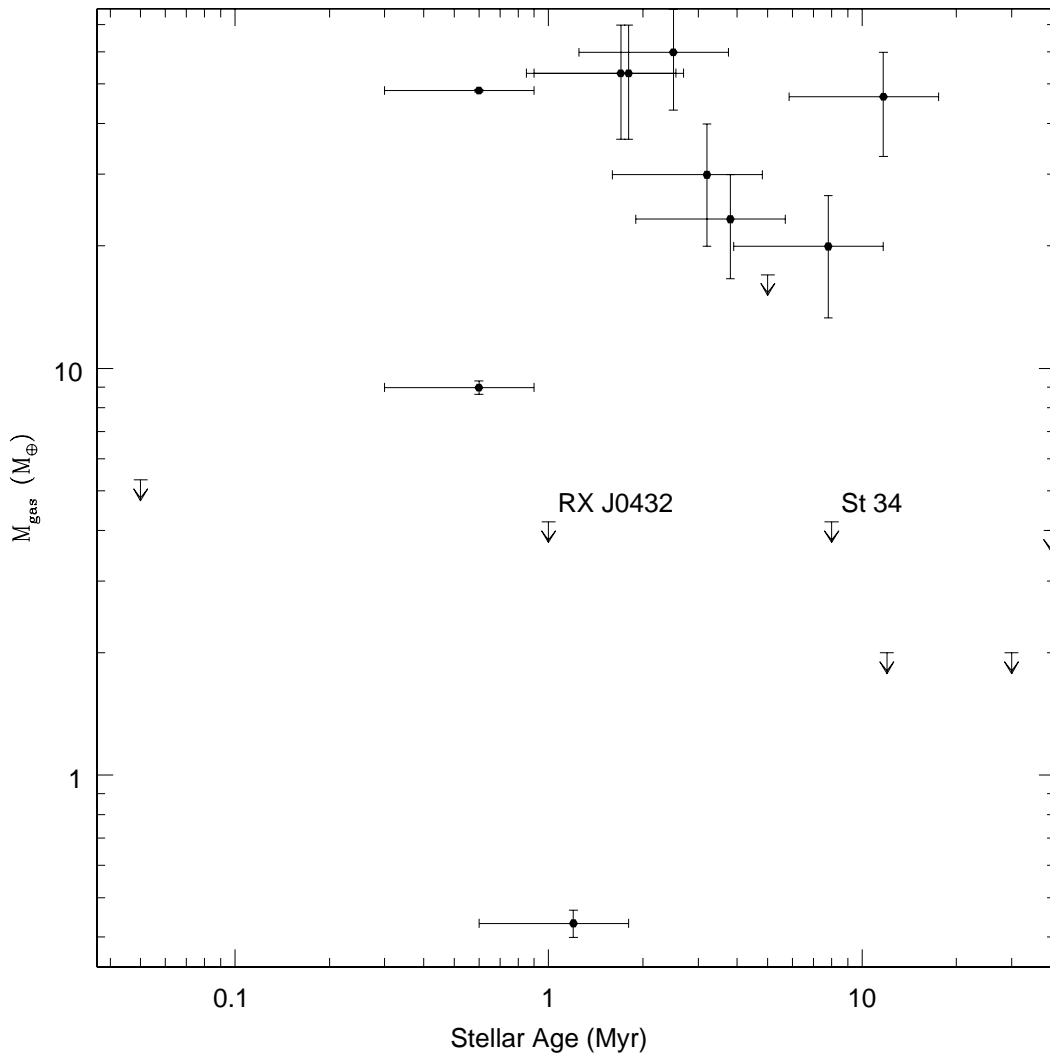
Fig. 2.— Gas circumstellar disk mass versus age of selected sources: our RX J0432.8+1735 and St 34 upper limits (*labeled*); upper limits from the Pascucci et al. (2006) sample (*unlabeled upper limits*) with ages ≤ 30 Myr (the Kelvin-Hemholtz contraction timescale for a 1 $M_\odot$ star); and exact mass determinations (*solid circles*) of BP Tau (^{13}CO $J = 2 - 1$; Dutrey et al. 2003); DL Tau, DO Tau (^{12}CO $J = 2 - 1$; Koerner & Sargent 1995); and DM Tau, DR Tau, GG Tau a, GM Aur, GO Tau, LkCa 15, RY Tau (^{12}CO $J = 3 - 2$ and ^{13}CO $J = 3 - 2$; Thi et al. 2001). We assume errors in stellar ages to be 50%.

RX J0432.8+1735, a WTTS of 1.0 ± 0.5 Myr, has disappeared quickly. Future observations of larger samples will be required to understand the diversity of disk lifetimes as a function of stellar properties.

REFERENCES

Alexander, R. D., Clarke, C. J., & Pringle, J. E. 2006, MNRAS, 369, 229

Andrews, S. M., Wilner, D. J., Hughes, A. M., Qi, C., & Dullemond, C. P. 2009, ApJ, 700, 1502

Armitage, P. J., & Clarke, C. J. 1996, MNRAS, 280, 458

Bary, J. S., Weintraub, D. A., & Kastner, J. H. 2003, ApJ, 586, 1136

Carkner, L., Feigelson, E. D., Koyama, K., Montmerle, T., & Reid, I. N. 1996, ApJ, 464, 286

D'Alessio, P., Merín, B., Calvet, N., Hartmann, L., & Montesinos, B. 2005, Revista Mexicana de Astronomia y Astrofisica, 41, 61

Dame, T. M., et al. 1987, ApJ, 322, 706

Damjanov, I., Jayawardhana, R., Scholz, A., Ahmic, M., Nguyen, D. C., Brandeker, A., & van Kerkwijk, M. H. 2007, ApJ, 670, 1337

D'Antona, F., & Mazzitelli, I. 1997, Memorie della Societa Astronomica Italiana, 68, 807

Downes, R. A., & Keyes, C. D. 1988, AJ, 96, 777

Dullemond, C. P., Hollenbach, D., Kamp, I., & D'Alessio, P. 2007, Protostars and Planets V, 555

Durisen, R. H., Boss, A. P., Mayer, L., Nelson, A. F., Quinn, T., & Rice, W. K. M. 2007, Protostars and Planets V, 607

Dutrey, A., Guilloteau, S., & Simon, M. 2003, A&A, 402, 1003

Dutrey, A., Guilloteau, S., & Ho, P. 2007, Protostars and Planets V, 495

Evans, N. J., II, et al. 2003, PASP, 115, 965

Fedele, D., van den Ancker, M. E., Henning, T., Jayawardhana, R., & Oliveira, J. M. 2009, arXiv:0911.3320

Gorti, U., & Hollenbach, D. 2009, ApJ, 690, 1539

Guilloteau, S., & Dutrey, A. 1994, A&A, 291, L23

Hartmann, L., et al. 2005, ApJ, 628, L147

Hughes, A. M., et al. 2010, arXiv:1007.3267

Ingleby, L., et al. 2009, ApJ, 703, L137

Jayawardhana, R., Hartmann, L., Fazio, G., Fisher, R. S., Telesco, C. M., & Piña, R. K. 1999, ApJ, 520, L41

Jensen, E. L. N. 1996, Ph.D. Thesis,

Kenyon, S. J., & Hartmann, L. 1995, ApJS, 101, 117

Koerner, D. W., & Sargent, A. I. 1995, AJ, 109, 2138

Kuznetsov, I. V., Fedoseev, L. I., & Shvetsov, A. A. 1982, Radiofizika, 25, 247

Mangum, J. G. 1993, PASP, 105, 117

Martín, E. L., & Magazzù, A. 1999, A&A, 342, 173

Meyer, M. R., et al. 2006, PASP, 118, 1690

Meyer, M. R., Backman, D. E., Weinberger, A. J., & Wyatt, M. C. 2007, Protostars and Planets V, 573

Meyer, M. R. 2009, IAU Symposium, 258, 111

Monin, J.-L., Clarke, C. J., Prato, L., & McCabe, C. 2007, Protostars and Planets V, 395

Najita, J. R., Carr, J. S., Glassgold, A. E., & Valenti, J. A. 2007, Protostars and Planets V, 507

Padgett, D. L., et al. 2006, ApJ, 645, 1283

Pascucci, I., et al. 2006, ApJ, 651, 1177

Qi, C., et al. 2004, ApJ, 616, L11

Roberge, A., Weinberger, A. J., Redfield, S., & Feldman, P. D. 2005, ApJ, 626, L105

Schlingman et al., in prep.

Scoville, N. Z., Sargent, A. I., Sanders, D. B., Claussen, M. J., Masson, C. R., Lo, K. Y., & Phillips, T. G. 1986, ApJ, 303, 416

Silverstone, M. D., et al. 2006, ApJ, 639, 1138

Skrutskie, M. F., et al. 1993, ApJ, 409, 422

Thébault, P., Marzari, F., Scholl, H., Turrini, D., & Barbieri, M. 2004, A&A, 427, 1097

Thi, W. F., et al. 2001, ApJ, 561, 1074

van Kempen, T. A., van Dishoeck, E. F., Brinch, C., & Hogerheijde, M. R. 2007, A&A, 461, 983

Webb, R. A., Zuckerman, B., Platais, I., Patience, J., White, R. J., Schwartz, M. J., & McCarthy, C. 1999, ApJ, 512, L63

White, R. J., & Hillenbrand, L. A. 2005, ApJ, 621, L65

Wichmann, R., et al. 2000, A&A, 359, 181